Mon. Not. R. Astron. Soc. **395,** L29–L33 (2009) doi:10.1111/j.1745-3933.2009.00635.x

Fast TeV variability in blazars: jets in a jet

Dimitrios Giannios,[1,2]★ Dmitri A. Uzdensky[1] and Mitchell C. Begelman[3,4]

[1]*Department of Astrophysical Sciences, Peyton Hall, Princeton University, Princeton, NJ 08544, USA*
[2]*Max Planck Institute for Astrophysics, Box 1317, D-85741 Garching, Germany*
[3]*Joint Institute for Laboratory Astrophysics, University of Colorado, Boulder, CO 80309, USA*
[4]*Department of Astrophysical and Planetary Sciences, University of Colorado, Boulder, CO 80309, USA*

Accepted 2009 January 31. Received 2009 January 28; in original form 2009 January 12

ABSTRACT

The fast TeV variability of the blazars Mrk 501 and PKS 2155−304 implies a compact emitting region that moves with a bulk Lorentz factor of $\Gamma_{\rm em} \sim 100$ towards the observer. The Lorentz factor is clearly in excess of the jet Lorentz factors $\Gamma_{\rm j} \lesssim 10$ measured on sub-pc scales in these sources. We propose that the TeV emission originates from compact emitting regions that move relativistically *within* a jet of bulk $\Gamma_{\rm j} \sim 10$. This can be physically realized in a Poynting flux-dominated jet. We show that if a large fraction of the luminosity of the jet is prone to magnetic dissipation through reconnection, then material outflowing from the reconnection regions can efficiently power the observed TeV flares through synchrotron-self-Compton emission. The model predicts simultaneous far-ultraviolet/soft X-ray flares.

Key words: radiation mechanisms: non-thermal – galaxies: active – BL Lacertae objects: individual: PKS 2155–304 – BL Lacertae objects: individual: Mrk 501 – gamma-rays: theory.

1 INTRODUCTION

There are two cases of blazars (Mrk 501 and PKS 2155−304) with flaring TeV emission that varies on time-scales of 3–5 min (Aharonian et al. 2007; Albert et al. 2007). This variability time-scale is much shorter than the light crossing time of the gravitational radius $t_{\rm lc} \sim$ hours of the supermassive black holes of these blazars (for inferred masses $M_{\rm BH} \sim 10^9\,{\rm M}_\odot$). This implies a very compact γ-ray emitting region. Furthermore, the fact that the TeV photons escape the production region implies that the emitting plasma moves with bulk $\Gamma_{\rm em} \gtrsim 50$ so as to avoid pair creation through interaction with soft radiation fields[1] (Begelman, Fabian & Rees 2008; Mastichiadis & Moraitis 2008). It therefore appears natural that a compact region within the blazar jet is the source of the TeV flares.

On the other hand, the jets of PKS 2155−304 and Mrk 501 have been resolved on sub-pc scales and show patterns that move with moderate Lorentz factor $\Gamma_{\rm j} \lesssim 10$ (Giroletti et al. 2004; Piner & Edwards 2004), much less than the one needed for TeV γ-rays to escape. This apparent contradiction can be avoided if, for some reason, the jet is efficiently decelerated on sub-pc scales (Georganopoulos & Kazanas 2003; Levinson 2007) after the TeV emission has taken place. The deceleration may be the result of radiative feedback in a spine/layer configuration (Ghisellini, Tavecchio & Chiaberge 2005; Tavecchio & Ghisellini 2008). Alternatively, finite opening angle effects in a $\Gamma_{\rm j} \sim 50$ jet can result in slow radio knot motions in blazars (Gopal-Krishna, Dhurde & Wiita 2004; Gopal-Krishna et al. 2007).

Here, we propose an alternative explanation for the origin of the TeV emission as a 'jets-in-a-jet' model. We argue that compact emitting regions that move relativistically *within* a jet of bulk $\Gamma_{\rm j} \sim 10$ can power the TeV flares. Ghisellini et al. (2009) proposed a similar basic idea of internal jet motions. We provide a different context/cause for these motions, arguing that they can be physically realized in a Poynting flux-dominated flow (PDF). We show that if a large fraction of the luminosity of a PDF is occasionally prone to magnetic dissipation through reconnection, then material outflowing at relativistic speed from the reconnection regions can efficiently power the observed TeV flares.

2 JETS-IN-A-JET MODEL

Consider a jet that moves radially with bulk $\Gamma_{\rm j}$, containing a blob of plasma with a characteristic Lorentz factor $\Gamma_{\rm co}$ at angle θ' with respect to the radial direction (measured in the jet rest frame). All primed/tilded quantities are measured in the rest frame of the jet/blob, respectively. In the lab frame, the blob moves with

$$\Gamma_{\rm em} = \Gamma_{\rm j}\Gamma_{\rm co}(1 + v_{\rm j}v_{\rm co}\cos\theta') \quad (1)$$

and at angle

$$\tan\theta = \frac{v_{\rm co}\sin\theta'}{\Gamma_{\rm j}(v_{\rm co}\cos\theta' + v_{\rm j})} \quad (2)$$

with respect to the radial direction. For a large range of angles of the order of $\theta' \sim \pi/2$, expressions (1) and (2) give $\Gamma_{\rm em} \sim \Gamma_{\rm j}\Gamma_{\rm co}$ and

★E-mail: giannios@astro.princeton.edu

[1] It is possible to relax the transparency constraint on the bulk Lorentz factor of the emitting region by supposing an extremely sharp lower cut off in the electron distribution (Boutelier, Henri & Petrucci 2008).

$\theta \sim 1/\Gamma_{\rm j}$. The blob moves with $\Gamma_{\rm em} \gg \Gamma_{\rm j}$ provided that the motions within the jet are relativistic. Such fast internal motions are possible in a PDF where magnetohydrodynamics (MHD) waves approach the speed of light.

2.1 The jet

For more quantitative estimates, we consider a jet with (isotropic) luminosity $L_{\rm j}$ that moves with the bulk $\Gamma_{\rm j}$. The jet is assumed to be strongly magnetized with Poynting-to-kinetic flux ratio (magnetization) $\sigma \gg 1$. As reference values, we use $\Gamma_{\rm j} = 10$ and $\sigma = 100$. The Poynting luminosity of the jet may be inferred from the flaring isotropic luminosity of PKS 2155−304 and is set to $L_{\rm j} = 10^{47}\,{\rm erg\,s^{-1}}$.

The energy density in the jet is (as measured in a frame comoving with the jet)

$$e'_{\rm j} = L_{\rm j}/4\pi r^2 c\Gamma_{\rm j}^2 = 12 L_{\rm j,47} r_2^{-2}\Gamma_{\rm j,1}^{-2} \quad {\rm erg\,cm^{-3}}, \tag{3}$$

where $A = 10^x A_x$ and the spherical radius is $R = rR_{\rm g}$ with $R_{\rm g} = 1.5 \times 10^{14}$ cm, corresponding to the gravitational radius of a black hole of 10^9 solar masses. The magnetic field strength in the jet is

$$B'_{\rm j} = \sqrt{4\pi e'_{\rm j}} = 12 L_{\rm j,47}^{1/2} r_2^{-1}\Gamma_{\rm j,1}^{-1} \quad {\rm Gauss}. \tag{4}$$

For a proton-electron jet, the particle number density in the jet is

$$n'_{\rm j} = B_{\rm j}^2/4\pi c^2 \sigma m_{\rm p} = 80 L_{\rm j,47} r_2^{-2}\Gamma_{\rm j,1}^{-2}\sigma_2^{-1}{\rm cm^{-3}}. \tag{5}$$

2.2 The emitting blob

We assume that a fraction of the magnetic energy of the jet is occasionally dissipated through reconnection. In the PDF considered here, current-driven instabilities are the most relevant ones in triggering the dissipation (e.g. Eichler 1993; Begelman 1998; Giannios & Spruit 2007; see, however, McKinney & Blandford 2009). Alternatively, reversals in polarity of the magnetic field that threads the black hole can lead to magnetic reconnection in the jet (see also Section 5).

Our picture for relativistic reconnection is the following (Lyubarsky 2005). High-σ material is advected into the reconnection region where the release of magnetic energy takes place. Part of the dissipated magnetic energy serves to give bulk acceleration of the 'blob' (in the rest frame of the jet) and the rest to heat the outflowing material to relativistic temperature. We explore the possibility that emission from the outflowing material produces the TeV flares, and refer to it as the 'emitting blob' or simply 'blob' (see Fig. 1).

For our quantitative estimates that follow, we adopt the relativistic generalization of Petschek-type reconnection worked out by Lyubarsky (2005; see also Watanabe & Yokoyama 2006 for relativistic MHD simulations that support this picture). In this model, the material leaves the reconnection region with bulk $\Gamma_{\rm co}$ close to the Alfvén speed of the upstream plasma $\Gamma_{\rm co} \sim \sqrt{\sigma} \simeq 10\sigma_2^{1/2}$ in the rest frame of the jet (Petschek 1964; Lyutikov & Uzdensky 2003; Lyubarsky 2005). For the last expression to be valid, we assume that the guide field (i.e. non-reversing field component) is not strong enough to affect the reconnection dynamics (i.e. $B'_{\rm guide} \lesssim B'_{\rm j}/\sqrt{\sigma}$; see also Section 5 for when this condition may be satisfied). As seen in the lab frame, plasma is ejected from the reconnection region with $\Gamma_{\rm em} \sim \Gamma_{\rm j}\Gamma_{\rm co} = 100\Gamma_{\rm j,1}\sigma_2^{1/2}$. The ratio of the thermal energy to rest mass in the blob frame is $\tilde{e}_{\rm em}/\tilde{\rho}_{\rm em}c^2 \sim \sqrt{\sigma}$, and reconnection leads to compression of the outflowing material $\tilde{\rho}_{\rm em} \sim \sqrt{\sigma}\rho'_{\rm j}$. The energy density in the blob is (Lyubarsky 2005)

$$\tilde{e}_{\rm em} \sim \sqrt{\sigma}\tilde{\rho}_{\rm em}c^2 \sim \sigma\rho'_{\rm j}c^2 = 12 L_{\rm j,47} r_2^{-2}\Gamma_{\rm j,1}^{-2} \quad {\rm erg\ cm^{-3}}. \tag{6}$$

The fact that this is similar to equation (3) is just a consequence of the pressure balance across the reconnection region.

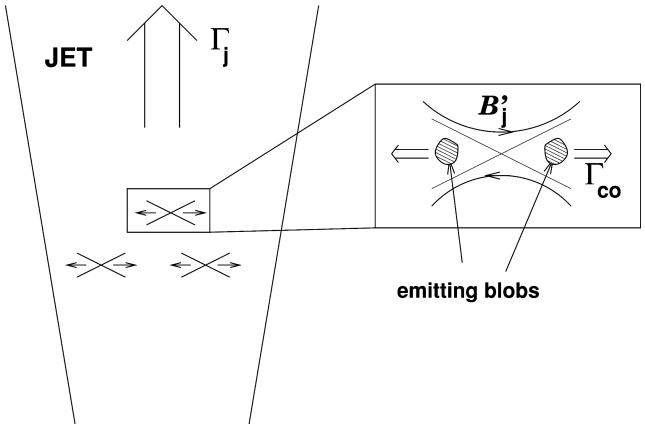

Figure 1. Schematic representation of the geometry of the 'jets in a jet' *shown in a frame comoving with the jet*. Right: the reconnection region enlarged. Plasma heated and compressed by magnetic reconnection leaves the reconnection region at relativistic speed $\Gamma_{\rm co} \gg 1$ within the jet in the form of blobs. Each blob emits efficiently through synchrotron-self-Compton in a narrow beam within the jet emission cone, powering a fast evolving soft X-ray and TeV flare. The sequence of flares seen in PKS 2155−304 may be the result of multiple reconnection regions or intrinsic instabilities (e.g. tearing) of one large reconnection region.

Even though we consider a PDF jet, the emitting (downstream) region is not necessarily magnetically dominated since a large part of the magnetic energy dissipates in the reconnection region. This has important implications for the radiative processes discussed below. On the other hand, the blob material may remain strongly magnetized. Any guide field in the reconnection region will be amplified by compression and will not dissipate. Lyubarsky (2005) shows that for a guide field $B'_{\rm guide} \lesssim B'_{\rm j}/\sqrt{\sigma}$, the magnetization of the blob (downstream plasma) is $\sigma_{\rm em} \lesssim 1$. The magnetic field in the blob rest frame is roughly estimated to be

$$\tilde{B}_{\rm em} \lesssim \sqrt{4\pi\tilde{e}_{\rm em}} = 12 L_{\rm j,47}^{1/2} r_2^{-1}\Gamma_{\rm j,1}^{-1} \quad {\rm Gauss}. \tag{7}$$

If electrons receive an appreciable fraction of the released energy $f \sim 0.5$, they are heated to characteristic

$$\gamma_{\rm e} \sim f\sqrt{\sigma} m_{\rm p}/m_{\rm e} \sim 10^4 f_{1/2}\sigma_2^{1/2}, \tag{8}$$

assumed to be isotropic in the blob rest frame.

2.2.1 The blob size

From the observed energy of the TeV flares, we can estimate the energy contained in each blob. Combined with the energy density (6), we derive an estimate of the size of the blob.

The TeV flares have observed (isotropic equivalent) luminosity $L_{\rm f} \sim 10^{47}\,{\rm erg\,s^{-1}}$ (allowing for a few times the observed energy to be emitted below ∼200 GeV, the low-energy threshold of the observations) and duration of $t_{\rm f} \sim 300$ s. The associated energy is then $E_{\rm f} = L_{\rm f} \times t_{\rm f} \simeq 3 \times 10^{49} L_{\rm f,47}\, t_{\rm f,300}$ erg.

In the model discussed here, the source of the flare moves with a bulk $\Gamma_{\rm em} \gg 1$. Its emission is concentrated in a cone that corresponds

to a fraction $\sim 1/4\Gamma_{\rm em}^2 = 2.5\times10^{-5}\ \Gamma_{\rm j,1}^{-2}\ \sigma_2^{-1}$ of the sky. The lab-frame energy (corrected for collimation) radiated from the blob is, thus, $E_{\rm rad} = E_{\rm f}/4\Gamma_{\rm em}^2 \simeq 7.5\times10^{44} L_{\rm f,47} t_{\rm f,300}\Gamma_{\rm j,1}^{-2}\sigma_2^{-1}$ erg. The energy contained in the blob is $E_{\rm em} = E_{\rm rad}/f$, where f stands for the radiative efficiency.[2] Combined with the energy density of the blob (6), the typical dimension of the blob is

$$\tilde{l} = (E_{\rm em}/\,\Gamma_{\rm em}\tilde{e}_{\rm em})^{1/3} \sim 10^{14}\,\frac{L_{\rm f,47}^{1/3} t_{\rm f,300}^{1/3} r_2^{2/3}}{\Gamma_{\rm j,1}^{1/3}\sigma_2^{1/2} f_{1/2}^{1/3} L_{\rm j,47}^{1/3}}\ {\rm cm}, \tag{9}$$

of the order of the size of the black hole. In the last expression we have assumed a quasi-spherical blob. The geometry of the emitting material may be much more complex, depending on the details of the reconnection geometry and whether the plasma radiates before it leaves the reconnection region or further downstream. In the latter case, a quasi-spherical emitter is more likely.

The emitting region cannot be arbitrarily large. Causality arguments for the emitting region limit its size to be smaller than $l' < \Gamma_{\rm em} c t_{\rm f} = 9\times10^{14}\Gamma_{\rm j,1}\sigma_2^{1/2} t_{\rm f,300}$ cm (e.g. Begelman et al. 2008). This can be cast as a 'causality' constraint to the bulk Lorentz factor of the jet (using also equation 9),

$$\Gamma_{\rm j} > 2\,\frac{r_2^{1/2} L_{\rm f,47}^{1/4}}{t_{\rm f,300}^{1/2}\sigma_2^{3/4} f_{1/2}^{1/4} L_{\rm j,47}^{1/4}}. \tag{10}$$

3 RADIATION MECHANISMS

The blob contains energetic electrons that emit though the synchrotron-self-Compton (SSC) and, possibly, external inverse Compton (EIC) mechanisms. Here, we explore the photon energies at which the different components are emitted, the radiative efficiency and under which conditions TeV emission can escape the source.

3.1 Synchrotron-self-Compton emission

The synchrotron emission of electrons with random Lorentz factor $\gamma_{\rm e}$ takes place at observed energy

$$\nu_{\rm syn} \simeq \Gamma_{\rm em}\gamma_{\rm e}^2\nu_{\rm c} \simeq 1.2 L_{\rm j,47}^{1/2}\sigma_2^{3/2} f_{1/2}^2 r_2^{-1}\ {\rm keV}, \tag{11}$$

where $\nu_{\rm c}$ is the electron cyclotron frequency. The peak of the self-Compton emission appears at

$$\nu_{\rm SSC} \simeq \gamma_{\rm e}^2\nu_{\rm syn} \simeq 120 L_{\rm j,47}^{1/2}\sigma_2^{5/2} f_{1/2}^4 r_2^{-1}\ {\rm GeV}, \tag{12}$$

with the scattering taking place in the Thomson limit.

While the synchrotron emission peaks in the soft X-ray band, the Comptonized component appears in the ∼100 GeV range. Any high-energy tail in the electron distribution powers the ∼TeV flares. For fast electron cooling (see below), the relative strength of the synchrotron and inverse Compton components depends on the ratio of the magnetic energy density to the radiation energy density in the emitting region. For magnetization of the downstream plasma (blob) of the order of unity and $f \sim 0.5$, the y-parameter in the emitting blob is $y \sim f\sigma_{\rm em}^{-1} \sim 1$. The cooling time-scale for the electrons in the blob rest frame is $\tilde{t}_{\rm cool} \simeq 5\times10^8/(1+y)\gamma_{\rm e}\tilde{B}_{\rm em}^2$ s or

$$\tilde{t}_{\rm cool} \simeq 1.8\times10^2\left(\frac{2}{1+y}\right)\frac{\Gamma_1^2 r_2^2}{L_{\rm j,47}\sigma_2^{1/2} f_{1/2}}\ {\rm s}. \tag{13}$$

[2] Assuming that the electrons are fast cooling; to be verified in the next section.

To evaluate whether there is efficient TeV emission, the cooling time is to be compared to the time it takes for the blob to be slowed down after it is ejected in the jet. The blob interacts with the rest of the jet plasma, and rarefaction and shock waves form that propagate in the blob with a speed $\sim c/2$ (for the relativistically hot, $\sigma_{\rm em} \lesssim 1$ blob under consideration). The blob slows down on a time-scale $\tilde{t}_{\rm s} \sim 2\tilde{l}/c$ as measured in its rest frame. Efficient TeV radiation takes place when $\tilde{t}_{\rm cool} < \tilde{t}_{\rm s}$, which can be cast as (using equations 9 and 13)

$$\Gamma_{\rm j} < 48\left(\frac{1+y}{2}\right)^{3/7}\frac{L_{\rm f,47}^{1/7} t_{\rm f,300}^{1/7} f_{1/2}^{2/7} L_{\rm j,47}^{2/7}}{r_2^{4/7}}. \tag{14}$$

The last expression implies that the blob can move with $\Gamma_{\rm em} \sim \Gamma_{\rm j}\,\sigma^{1/2} \sim 100$ or larger (for $\sigma \sim 100$) and still be in a fast SSC cooling regime, in contrast to expectations from uniformly moving jets (Begelman et al. 2008). This is a result of the compression that takes place in the reconnection layer, allowing for higher magnetic energy density and shorter cooling time-scale compared to those of a jet that moves uniformly with $\Gamma_{\rm j} \sim 100$.

Pair production on synchrotron photons might prevent ∼1 TeV photons from escaping the blob. The energy density of synchrotron photons is at most that of the heated electrons $\tilde{e}_{\rm syn} \sim f\tilde{e}_{\rm em} \sim 6 L_{\rm j,47} f_{1/2} r_2^{-2}\Gamma_1^{-2}\ {\rm erg\,cm^{-3}}$, while the bulk of the emission takes place at energy $\tilde{\nu}_{\rm syn} \sim \gamma_{\rm e}^2\nu_{\rm c} \sim 12 L_{\rm j,47}^{1/2}\sigma_2 f_{1/2}^2 r_2^{-1}\Gamma_{\rm j,1}^{-1}$ eV (in the rest frame of the blob). The comoving number density of photons at the peak of the synchrotron emission is

$$\tilde{N}_{\rm syn}^{\rm peak} \simeq \tilde{e}_{\rm syn}/h\tilde{\nu}_{\rm syn} = 3.2\times10^{11}\,\frac{L_{\rm j,47}^{1/2}}{\sigma_2 f_{1/2} r_2\Gamma_1}\ {\rm ph\,cm^{-3}}. \tag{15}$$

Most of the target photons that annihilate with the ∼1 TeV γ-rays are close to the pair-creation threshold, i.e. at $\tilde{\nu}_{\rm target} \sim 0.6\Gamma_{\rm em}$ eV $= 60\Gamma_1\sigma_2^{1/2}$ eV, typically above the bulk of the synchrotron emission. Assuming conservatively a fast cooling spectrum $f_\nu \sim \nu^{-1}$ between $\tilde{\nu}_{\rm syn}$ and $\tilde{\nu}_{\rm target}$, the number density of the target photons is a factor of $\sim(\tilde{\nu}_{\rm syn}/\tilde{\nu}_{\rm target})$ smaller than that at the peak frequency. Applying the last correction factor to equation (15), we estimate

$$\tilde{N}_{\rm syn}^{\rm target} = 6.3\times10^{10}\,\frac{L_{\rm j,47} f_{1/2}}{\sigma_2^{1/2} r_2^2\Gamma_1^3}\quad {\rm ph\,cm^{-3}}. \tag{16}$$

As the TeV γ-rays cross the blob, they encounter optical depth to pair creation of

$$\tau_{\gamma\gamma} \simeq \sigma_T\tilde{N}_{\rm syn}^{\rm target}\tilde{l}/5 = 0.83\,\frac{L_{\rm f,47}^{1/3} t_{\rm f,300}^{1/3} L_{\rm j,47}^{2/3} f_{1/2}^{2/3}}{\sigma_2 r_2^{4/3}\Gamma_1^{10/3}}. \tag{17}$$

From the last expression, we obtain the condition that $\tau_{\gamma\gamma} < 1$ is satisfied for jet bulk Lorentz factor

$$\Gamma_{\rm j} > 9\,\frac{L_{\rm f,47}^{1/10} t_{\rm f,300}^{1/10} L_{\rm j,47}^{1/5} f_{1/2}^{1/5}}{r_2^{2/5}\sigma_2^{3/10}}. \tag{18}$$

This limit is much less stringent than the one ($\Gamma_{\rm j} > 50$) found in homogeneous jet models (Begelman et al. 2008; Mastichiadis & Moraitis 2008). This moderate value of $\Gamma_{\rm j}$ can be easily reconciled with values inferred by the radio observations (e.g. Foschini et al. 2007) and unification schemes for active galactic nuclei jets.

We conclude that there is a reasonably wide range of Lorentz factors of the jet, bounded by the expressions (14) and (18), for which the SSC mechanism emits efficiently in the ∼100 GeV-TeV range and the emission escapes the source. The 'causality' constraint for the Lorentz factor of the source (10) is also satisfied.

3.2 External inverse Compton emission

EIC may also contribute to the γ-ray emission and to the opacity for the γ-rays. It is, however, not necessary for efficient TeV emission in our model. For the EIC mechanism to dominate the SSC, the energy density of external soft photons must exceed that of the magnetic field in the rest frame of the blob. The lab-frame energy density of the external radiation must be

$$U_{\rm soft} > 6\times10^{-4}\frac{L_{\rm j,47}f_{1/2}}{\Gamma_1^4\sigma_2 r_2^2\sigma_2^{3/10}}\,{\rm erg\,cm^{-3}}. \quad (19)$$

This is too high to be attributed to the accretion disc (see also Begelman et al. 2008). We cannot exclude, however, a powerful external source of soft photons that is located in the vicinity of the hot blob. This source may provide additional soft photons to be upscattered to the ∼TeV range.

4 STATISTICS OF FLARES

In the 'jets-in-a-jet' model discussed here, the emitting region moves with large bulk $\Gamma_{\rm em}\sim100$. The emission from the blob is beamed into a narrow cone $\Delta\Omega_{\rm em}\sim1/4\Gamma_{\rm em}^2\sim2.5\times10^{-5}\Gamma_{\rm j}^2\sigma_2$ of the sky and is directed at an angle $\theta\sim1/\Gamma_{\rm j}$ with respect to the radial direction (see equation 2). The TeV emission is beamed within the cone where the bulk of the jet emission takes place.

Assuming that the jet opening angle is $\theta_{\rm j}\sim1/\Gamma_{\rm j}$ and that the jet points at us, the probability to see the emission from a single blob is $P\sim\Delta\Omega_{\rm em}/\Delta\Omega_{\rm j}\sim1/100\sigma_2$. Observationally, the duty cycle of the flaring activity is low, maybe of the order of $\sim10^{-2}$. On the other hand, when it occurs, it is characterized by several flares on ∼1 hour time-scales (e.g. Aharonian et al. 2007). So one needs to account for flares repeating on time-scales of $t_{\rm rep}\sim10^3t_{\rm f,300}$ s.

If the emitting blobs are oriented randomly (in the rest frame of the jet), then correcting for the blobs that are not emitting towards the observer, the rate of dissipation events in the jet during the flaring activity is $\sim1/Pt_{\rm rep}\sim0.1\sigma_2t_{\rm f,300}^{-1}\,{\rm s^{-1}}$. The rate of dissipation of energy in the blobs corresponds to a significant fraction of the jet power. Every blob contains lab-frame energy $E_{\rm em}=1.5\times10^{45}L_{\rm f,47}$ $t_{\rm f,300}\Gamma_1^{-2}\sigma_2^{-1}f_{1/2}^{-1}$ erg (see Section 2.2.1). The rate of dissipation in the jet is $L_{\rm diss}=E_{\rm em}/Pt_{\rm rep}\simeq1.5\times10^{44}L_{\rm f,47}\Gamma_1^{-2}f_{1/2}^{-1}\,{\rm erg\,s^{-1}}$. The (corrected for beaming) luminosity of the jet is $L_{\rm j}^{\rm cor}\simeq L_{\rm j}\theta_{\rm j}^2/4\sim L_{\rm j}/4\Gamma_{\rm j}^2\simeq2.5\times10^{44}L_{\rm j,47}\Gamma_1^{-2}\,{\rm erg\,s^{-1}}$. The dissipated fraction of the jet luminosity is of the order of unity: $L_{\rm diss}/L_{\rm j}^{\rm cor}\simeq0.6L_{\rm f,47}L_{\rm j,47}^{-1}f_{1/2}^{-1}$.

On the other hand, it is just as likely that the short-time variability is produced by intrinsic instabilities (e.g. tearing) of one large reconnection region. In this case, one large (1 hour long) flare involves the ejection of several individual plasmoids. Because their motion is controlled by the large-scale magnetic field, the directions of these blobs will no longer be random, but instead will be strongly correlated with each other; this will significantly lessen the flare energetic requirements.

Although we have focused on the fastest evolving flares in blazars, which are the most constraining for the model, the same mechanism may be responsible for the observed variability on longer (∼hours) time-scales. The longer time-scales may be due to larger emitting regions and/or longer cooling time-scales of the electrons. Both of these conditions are likely to be met at larger distances from the black hole. Maybe the shortest variability comes from the reconnection regions associated with polarity inversions of the magnetic field that threads the black hole (which might naturally have a scale set by the size of the black hole) while the longer term variability could be associated with current-driven instabilities that develop in the jet at larger distance.

5 DISCUSSION/CONCLUSIONS

In this Letter, we propose a jets-in-a-jet model as a plausible source of the TeV flares in Mrk 501 and PKS 2155−304. We postulate the existence of blobs that move relativistically within the jet. These can result in fast-evolving flares and an environment transparent to γ-rays even for a jet with moderate $\Gamma_{\rm j}\sim10$, much easier reconciled with bulk Lorentz factors inferred from pc-scale observations (Giroletti et al. 2004; Piner & Edwards 2004; Piner, Pant & Edwards 2008) than models invoking higher-Γ jets.

The jets in a jet can be realized in a PDF where a fraction of the jet luminosity is dissipated in reconnection events. Material leaves the reconnection site at relativistic speed, as measured in the jet frame, while the liberated energy can power bright flares through the synchrotron-self-Compton mechanism.[3] The synchrotron component appears in the soft X-rays and the inverse Compton in the ∼100 GeV-TeV range. Simultaneous X-ray observations may have already revealed indications of such a TeV–X-ray correlation (Albert et al. 2007). The model prediction of simultaneous X-ray flares assumes that most of the X-rays come from the flaring sites, but there could be other, slowly varying regions that produce X-rays as well, perhaps further out so the photon densities are lower and pair production is not too large. For example, the X-rays could also be produced in magnetically dominated regions that result in little TeV emission.

The mechanism presented here has similarities to a mechanism proposed for the variability of the prompt emission of GRBs, i.e. it can be enhanced by relativistic motions within the GRB jet. Such motions may result from magnetic dissipation (Blandford 2002; Lyutikov 2006a,b) or relativistic turbulence (Narayan & Kumar 2008).

Ghisellini et al. (2008) proposed to explain the rapid TeV variability of Mrk 501 and PKS 2155−304 via the localized magneto-centrifugal acceleration of beams of electrons. In their model, the particles stream along the magnetic field lines at very small pitch angles, resulting in negligible synchrotron emission and 'orphan' TeV flares. The presence or absence of simultaneous X-ray flares may be used to discriminate between the two models.

Although the jet is Poynting flux-dominated, this is not necessarily the case for the material that leaves the reconnection region which powers the flares. The magnetization in this region is expected to be much lower than that of the bulk of the jet. Inferring the magnetization of the jet by modelling the TeV flares (as done, e.g., by Ghisellini & Tavecchio 2008) may be misleading in the context of the model presented here.

The energy that is dissipated during the flaring activity is a significant fraction of that of the jet, indicating that we are dealing with an efficient dissipation event. For the parameters adopted here ($\Gamma_{\rm j}\sim10$, magnetization in the jet $\sigma\sim100$), the dissipation could take place near or just outside the Alfvén radius of a jet that is ejected with an initial Michel magnetization parameter $\mu\sim\Gamma_{\rm j}\sigma\sim1000$ (Michel 1969; Begelman & Li 1994). In this region, the flow may be particularly prone to (kink-type) current-driven instabilities (e.g. Eichler 1993; Begelman 1998; Giannios & Spruit 2007) that are currently being investigated by three-dimensional MHD

[3] A similar mechanism has been proposed by Giannios (2006) for the X-ray flares seen in the afterglow of gamma-ray bursts (GRBs).

simulations (e.g. Moll, Spruit & Obergaulinger 2008; McKinney & Blandford 2009) and may provide a plausible trigger for magnetic dissipation. Alternatively, efficient dissipation may result from reversal of the polarity of the magnetic field that threads the black hole. If the reversal takes place on the light crossing time-scale of the black hole $\sim R_g/c$, then parts of the jet with antiparallel magnetic fields can collide at $R \sim \Gamma_j^2 R_g \sim 100 R_g$, dissipating Poynting flux through reconnection at the location of the collision.

Since the jet under consideration is ejected with $\mu \sim 1000$, it can be, in principle, accelerated to terminal Lorentz factors as high as $\Gamma_j \sim 1000$. This does not appear to happen in blazars. On the other hand, GRB jets do attain these high Lorentz factors. If the jets in the two sources are launched with similar magnetization, the difference in the acceleration efficiency may be understood by the difference in the confining external medium (Komissarov et al. 2008; Tchekhovskoy, McKinney & Narayan 2008). Recent relativistic MHD simulations (Komissarov et al. 2009; see also Tchekhovskoy et al. 2008 for force-free simulations) show that if the pressure of the external medium provides a collimating funnel, the acceleration is efficient, in contrast to the case of a less collimating external pressure. It is possible that the collapsing star provides such external pressure to the GRB jet. The absence of similar confinement in blazars might account for the difference in the acceleration efficiency.

ACKNOWLEDGMENTS

We thank the referee, Gabriele Ghisellini, for insightful comments that greatly improved the manuscript. DG acknowledges support from the Lyman Spitzer Jr Fellowship awarded by the Department of Astrophysical Sciences at Princeton University. DAU is supported by National Science Foundation grant no. PHY-0215581 (PFC: Center for Magnetic Self-Organization in Laboratory and Astrophysical Plasmas). MCB acknowledges support from NASA, via a *Fermi Gamma-ray Observatory* Guest Investigator grant.

REFERENCES

Aharonian F. et al., 2007, ApJ, 664, L71
Albert J. et al., 2007, ApJ, 669, 862
Begelman M. C., 1998, ApJ, 493, 291
Begelman M. C., Li Z.-Y., 1994, ApJ, 426, 269
Begelman M. C., Fabian A. C., Rees M. J., 2008, MNRAS, 384, L19
Blandford R. D., 2002, in Gifanov M., Sunyaev R., Churazov E., eds, Lighthouses of the Universe: the Most Luminous Celestial Objects and their Use for Cosmology. Springer, Berlin, p. 381
Boutelier T., Henri G., Petrucci P. O., 2008, MNRAS, 390, L73
Eichler D., 1993, ApJ, 419, 111
Foschini L. et al., 2007, ApJ, 657, L81
Georganopoulos M., Kazanas D., 2003, ApJ, 589, L5
Ghisellini G., Tavecchio F., 2008, MNRAS, 386, L28
Ghisellini G., Tavecchio F., Chiaberge M., 2005, A&A, 432, 401
Ghisellini G., Tavecchio F., Bodo G., Celotti A., 2009, MNRAS, 393, L16
Giannios D., 2006, A&A, 455, L5
Giannios D., Spruit H. C., 2007, A&A, 469, 1
Giroletti M. et al., 2004, ApJ, 600, 127
Gopal-Krishna, Dhurde S., Wiita P. J., 2004, ApJ, 615, L81
Gopal-Krishna, Dhurde S., Sircar P., Wiita P. J., 2007, MNRAS, 377, 446
Komissarov S., Vlahakis N., Konigl A., Barkov M., 2009, MNRAS, in press (doi:10.1111/j.1365-2966.2009.14410.x) (arXiv:0811.1467)
Levinson A., 2007, ApJ, 671, L29
Lyubarsky Y. E., 2005, MNRAS, 358, 113
Lyutikov M., 2006a, MNRAS, 369, L5
Lyutikov M., 2006b, New J. Phys., 8, 119
Lyutikov M., Uzdensky D., 2003, ApJ, 589, 893
McKinney J. C., Blandford R. D., 2009, MNRAS, 394, L126
Mastichiadis A., Moraitis K., 2008, A&A, 491, L37
Michel F. C., 1969, A&A, 158, 727
Moll R., Spruit H. C., Obergaulinger M., 2008, A&A, 492, 621
Narayan R., Kumar P., 2008, MNRAS, 394, L117
Petschek H. E., 1964, in Ness W. N., ed., NASA SP-50, The Physics of Solar Flares. NASA Science and Technical Information Division, Washington DC, p. 425
Piner B. G., Edwards P. G., 2004, ApJ, 600, 115
Piner B. G., Pant N., Edwards P. G., 2008, ApJ, 678, 64
Tavecchio F., Ghisellini G., 2008, in Aharonian F. A., Hofmann W., Rieger F., eds, AIP Conf. Proc. Vol. 1085, High Energy Gamma-Ray Astronomy. Am. Inst. Phys., New York, p. 431
Tchekhovskoy A., McKinney J. C., Narayan R., 2008, MNRAS, 388, 551
Watanabe N., Yokoyama T., 2006, ApJ, 647, L123

This paper has been typeset from a TEX/LATEX file prepared by the author.